Available online at www.sciencedirect.com

ScienceDirect

Ceramics International 40 (2014) 281–287

CERAMICS INTERNATIONAL

www.elsevier.com/locate/ceramint

Structure and antibacterial property of nano-SiO_2 supported oxide ceramic

Nasrin Talebian*, Elham Zare

Science Faculty, Department of Chemistry, Shahreza Branch, Islamic Azad University, Razi Chemistry Research Centre, Women Research Council, 86145-311 Shahreza, Isfahan, Iran

Received 31 March 2013; received in revised form 23 May 2013; accepted 24 May 2013
Available online 18 June 2013

Abstract

SiO_2 doped samples with different cobalt loading and pure SiO_2 and Co_3O_4 nanopowders were synthesized by the solvothermal method and their antibacterial activities were studied. The morphology and crystallinity of the powders were analyzed by scanning electron microscopy and X-ray diffractometry patterns, respectively. The increase of particle size with doping concentration was obtained for cobalt-doped samples. The optical properties were studied using UV–vis spectroscopy. Optical studies showed a blue shift in the absorbance spectrum with increasing the doping concentration. The antibacterial activities of undoped SiO_2, Co-doped SiO_2 and pure Co_3O_4 nanoparticles against a Gram-negative bacterium *Escherichia coli* (*E. coli*, ATCC 25922) and a Gram-positive bacterium *Staphylococcus aureus* (*S. aureus*, ATCC 29213) were investigated under UV illumination and in the dark condition. Bactericidal effects were determined by the minimum inhibitory concentration (MIC) method. There was no activity for pure SiO_2 and Co_3O_4, however, cobalt doping significantly improved antibacterial activity against both bacteria. Bacterial growth inhibition was observed under dark condition with lower efficiency than under UV illumination. The antibacterial efficiencies were affected by the physiological status of the bacterial cells, different morphologies, particle sizes and optical properties of samples.

Keywords: Nano-SiO_2 carrier; Co_3O_4 nanostructure; Solvothermal method; Antibacterial activity

1. Introduction

Bacterial contamination and growth in water are potential health hazards demanding disinfection. Moreover, the food-borne diseases still remain a universal problem [1] in spite of the rapid growth of nanotechnology as a possible approach to reduce the microbial contamination on food surfaces and in food preparation environments. The *Staphylococcus aureus* is a leading cause of gastroenteritis resulting from the consumption of contaminated food. On the other hand, certain types of *Escherichia coli* cause foodborne illness. The majority of bacteria recovered from different types of food and environmental sources have been found resistant to at least one antimicrobial drug [2]. Therefore, three types of antibacterials including metals, metal oxides and organic polymers were recently developed. However, new research has attracted interest in antibacterial nanomaterial containing various inorganic substances compared to the organics, due to their improved safety and stability [3,4]. Among these, ceramics with inherent bactericidal activity are convenient to use as they are insoluble.

Some antibacterial agents, when loaded onto inorganic carrier and released from it slowly by design, act as inorganic disinfectants, which are superior in terms of safety, durability and heat resistance compared with conventional organic ones [5]. As for inorganic carriers, some compounds such as zeolite [6], phosphate [7], titanium dioxide [8], activated carbon [9], montmorillonite [10], water-soluble glass [11] and mesoporous silica [12] have been investigated.

Nano-SiO_2 particles are expected to be one of the most promising carriers suitable for development of high performance antibacterial and bactericidal materials due to following reasons: (1) nano-SiO_2 particles are of extremely high surface activity and porous structure resulting to sufficient adsorption properties; (2) nanometric size particle metals/or metal oxides embedded in silica matrix have the lower tendency to agglomerate; (3) silica matrix is chemically inert,

*Corresponding author. Tel.: +98 321 329 2260; fax: +98 321 3232701.
E-mail addresses: nasrin_talebian@yahoo.com, talebian@iaush.ac.ir (N. Talebian).

0272-8842/$ - see front matter © 2013 Elsevier Ltd and Techna Group S.r.l. All rights reserved.
http://dx.doi.org/10.1016/j.ceramint.2013.05.135

biocompatible and resistant to microbial attack both in vitro and in vivo and (4) controlled release of nanoparticles from SiO_2 matrix. These are the reasons why the development of inorganic bactericide and disinfectant prepared by loading antibacterial agents onto silica matrix carrier is receiving extensive attention for application in domestic and industrial fields [13,14].

The wide investigations on the antibacterial effect of various nanostructured systems including doped metal oxides [15], metal loaded silica [16] and composites [17] have been carried out. Nevertheless, the reports on the cobalt-included bactericides are limited to Co-doped nanoparticles [18,19], and cobalt coordination complexes in oxidation state 3+ [20]. As reported previously, no significant antibacterial activity was observed for cobalt oxides [21].

To our knowledge, for the first time we report the toxicity of Co-doped SiO_2 nanostuctures. This study examines the effects of Co-doping concentration and exposure time on the growth of the bacteria. In this paper, bactericidal nano-SiO_2 specimens were synthesized by solvothermal reaction. Among solution-based methods for tailored nanomaterials synthesis, solvothermal synthesis are related to homogeneous novel nucleation processes due to the elimination of the calcination step, producing very low grain sizes and high-purity powders [22]. The structure, morphologies and optical properties of the all samples were determined by X-ray diffraction (XRD), scanning electron microscopy (SEM) and UV–vis spectroscopy. Chemical compositions of the prepared samples were estimated by chemical analysis. Their antibacterial properties were also examined against *Escherichia coli* (*E. coli*, ATCC 25922) and *Staphylococcus aureus* (*S. aureus*, ATCC 29213).

2. Materials and methods

2.1. SiO_2 supported oxide ceramic synthesis

Two sols were separately prepared using tetraethyl orthosilicate (TEOS, $Si(OC_2H_5)_4$), and cobalt nitrate (Co $(NO_3)_2 \cdot 6H_2O$) as sources of Si and Co, respectively. For SiO_2 synthesis, TEOS and distilled water were mixed and stirred at room temperature. Then, 0.5 M HNO_3 solution was added as hydrolysis catalysis and to control the pH value at 3. $Co(NO_3)_2 \cdot 6H_2O$ was separately dissolved in 30 ml of H_2O and ethanol mixture with magnetic stirring for at least 30 min to form a red solution. One part of each set was left unmixed to prepare single component Co_3O_4 and SiO_2 powders. To the remaining Si sol, requisite amounts of Co sol prepared were added to obtain three sols at 10, 30 and 50% Co-doped SiO_2, individually. The sols were further stirred for 2 h at room temperature. Then, each sol was transferred into an individual 80 ml autoclave with a Teflon liner and heated at 180 °C for 20 h. The resulting products were filtered and washed several times with distilled water and ethanol, then, dried at 100 °C for 1 h, and finally annealed in the air atmosphere at 450 °C for 3 h.

2.2. Characterization

Powder X-ray diffraction (XRD) patterns were obtained by using a Bruker D8 Advance X-ray diffractometer with Cu Kα radiation ($\lambda = 1.5418$ Å). The size and morphology of all the catalysts were examined with a Philips, XL30 scanning electron microscope (SEM). The composition of the doped powders was analyzed by electron dispersive X-ray analysis (EDS). The optical properties were performed on a Shimadzu, MPC-2200 UV–vis spectrophotometer operated over the range of 200–800 nm at a resolution of 2.0 nm.

2.3. Antibacterial activity

The antibacterial activities of undoped SiO_2, Co-doped SiO_2 and Co_3O_4 nanoparticles were investigated against a Gram-negative bacterium *E. coli* and a Gram-positive bacterium *S. aureus* under UV illumination and in the dark condition. Nutrient broth (NB) was used as a growing medium for both the microorganisms at 37 °C for 20 h. The culture solution was centrifuged, and the cells were washed and suspended in distilled water, reaching a final concentration of 10^5 cells/ml *E. coli* or *S. aureus*. We used minimal inhibitory concentrations (MIC) method to test the antimicrobial activity. The MIC is the lowest concentration of an antimicrobial material that will inhibit the visible growth of a microorganism after incubation. Four different concentrations (0, 1, 3 and 6 μg/ml) of the Co-doped SiO_2 nanostructures have been used in the present study to determine the MIC. For single component SiO_2 and Co_3O_4 powders, the constant concentration of 6 μg/ml was used. The certain amounts of each sample were put into above suspended solution to keep in contact with *E. coli* or *S. aureus* respectively, and shaken at 37 °C (dark condition)/ or illuminated under four 8 W UV lamps (Philips UV-A, $\lambda_{max} = 365$ nm) for up to 56 h. Aliquots of 0.1 ml of each mixture (water+bacterium) were sampled every 4 h. These aliquots were diluted in distilled water. Each group of samples was spread on NB agar plates and incubated at 37 °C for 24 h, respectively. The number of viable cells in the each sample was determined by choosing the appropriate dilution of the sample onto NB agar plates and counting colonies that appeared on the plates.

3. Results and discussion

3.1. Structure and morphology

Fig. 1 shows typical comparative X-ray diffraction patterns for single SiO_2, single Co_3O_4 and Co-doped samples, respectively. SiO_2 XRD pattern indicated amorphous phase. All the XRD patterns of Co-doped SiO_2 and single Co_3O_4 samples are commonly in good accord with those of cubic Co_3O_4. The (111), (220), (311), (400), (511) and (440) planes for Co_3O_4 are assigned on the peaks. At higher Co doping concentration, some new XRD peaks appear, possibly due to improved crystallinity. The particle size increases at higher Co doping concentration (table 1). The surface morphology of the samples was investigated by SEM as shown in Fig. 2. There

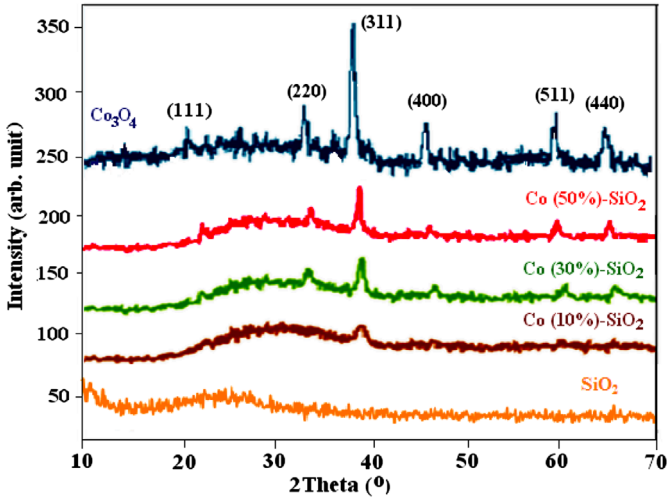

Fig. 1. X-ray diffraction patterns of the Co-doped SiO_2, pure SiO_2 and Co_3O_4 samples.

Table 1
Particle size and band gap of samples.

Sample	Particle size	Band gap (eV)
SiO_2	47	—
Co (50%)-SiO_2	68	3.08
Co (30%)-SiO_2	56	3.10
Co (10%)-SiO_2	42	3.14
Co_3O_4	87	3.10 (1.56)

was smooth distribution of nanoparticles for doped samples compared to single Co_3O_4 one that showed some aggregation. The composition of the powders was confirmed by EDS analysis and is shown in Fig. 3. The elemental ratio for doped samples was found to be consistent with the molar ratios of the precursors used.

3.2. UV–visible absorption spectra and energy band gap measurements

Fig. 4 shows the absorption spectra of the single and doped samples. It is clear from figure that there are two distinct characteristics for Co-doped SiO_2 samples compared to single SiO_2: the higher molar adsorption and the shift toward longer wavelengths. The optical band gap values were reported in Table 1 and decreased at higher Co doping level for doped samples. Two E_g values for single Co_3O_4 sample are obtained, 3.11 and 1.52 eV. As previously reported [23], the first band gap can be assigned to O^{2-}–Co^{2+} charge transfer process (basic optical band gap energy, or valence to conduction band excitation) while the second one to O^{2-}–Co^{3+} charge transfer process (Co^{3+} level is located below the conduction band).

3.3. Antibacterial properties

The antimicrobial activity of the samples was determined by colony count method using Gram negative *E. coli* and Gram positive *S. aureus* exposed to different samples to assess their bactericidal effect under UV light and dark conditions as the

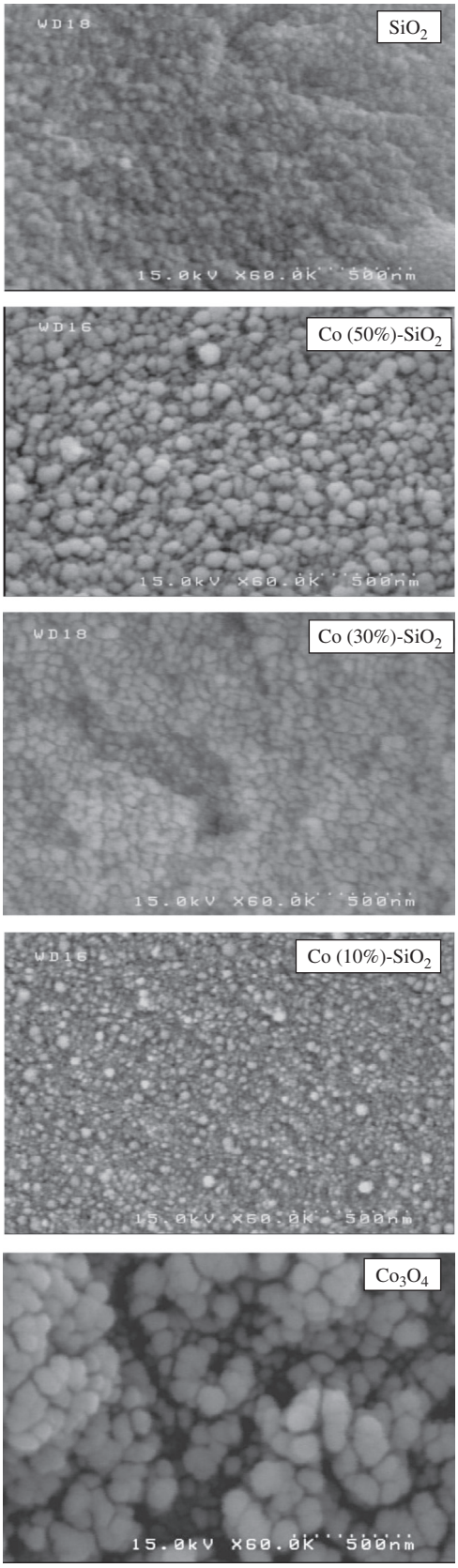

Fig. 2. SEM micrographs of the samples.

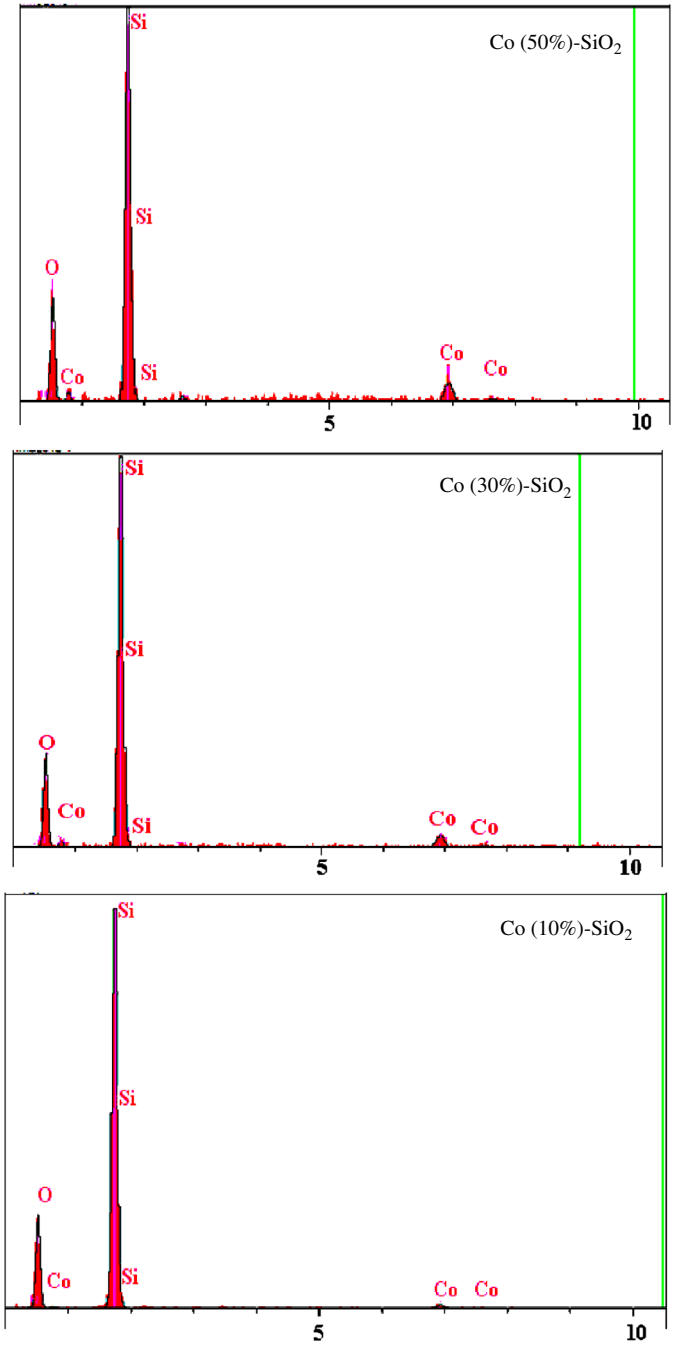

Fig. 3. The composition of the Co-doped samples by EDS analysis.

test cultures. For catalytic toxicity, many factors are important including size, chemical composition, structural and optical characteristics of catalyst and microorganism type as discussed below.

3.3.1. Effects of the catalyst chemical composition

Fig. 5 shows the growth/no growth of *E. coli* bacteria that were treated with 6 μg/ml concentrations of each catalyst spreading on agar plates for single powders only under UV illumination, but under UV illumination and in the dark condition for Co-doped samples. No efficient activity was observed for single SiO_2 and Co_3O_4 powders at all. No

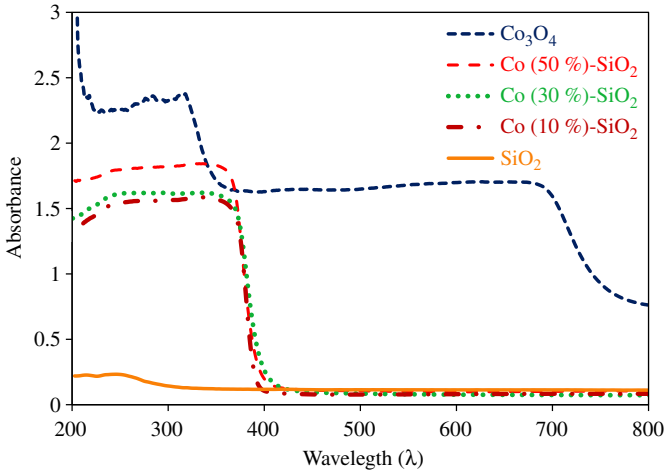

Fig. 4. The absorption spectra of the different samples.

significant decrease in CFU (colony-forming unit) in the Co-doped nanoparticle free medium was also observed after UV light exposure (not shown in Fig. 5). This indicates that the photochemical inactivation was negligible under UV-A irradiation with low energy. Co-doped SiO_2 samples have demonstrated effective toxicity against both the Gram-positive *S. aureus* and Gram-negative *E. coli* strains. At higher Co-doping level, the growth inhibition has been occurred more efficient. The highest activity was observed for sample Co (50%)-SiO_2 and followed order Co (50%)-SiO_2 > Co (30%)-SiO_2 > Co (10%)-SiO_2. These results indicated that the silica as inorganic carrier could activate the Co_3O_4 nanoparticles. There are some reports on the improved antibacterial activity using silica supported bactericide agents [24]. However, this is first results about construction of Co_3O_4 nanoparticle activity using silica as inorganic carrier.

3.3.2. Influence of catalyst particle size

The particle size may play a critical role in the biocide activity of nanoparticle catalyst. However, contradictory results about the impact of particle size on the catalytic activity of nanoparticles have been reported [25,26]. As shown in Fig. 5, it was found that the antibacterial activity of samples increased with increasing particle size (nm) in order of Co (50%)-SiO_2 (68) > Co (30%)-SiO_2 (56) > Co (10%)-SiO_2 (42). The higher crystallinity may improve the separation efficiency of photoinduced electron–hole pairs which results to more efficient reactive oxygen species production as the major species in the photocatalytic inactivation.

3.3.3. Effect of the catalyst photoresponse

There was an inverse relationship between band gap energy and biocide activity of Co-doped SiO_2 samples. A decrease in band-gap energy for sample Co (50%)- SiO_2 results in the higher spectral response. The photocatalytic activity could be affected by a change in photon harvesting depending on the band gap energy.

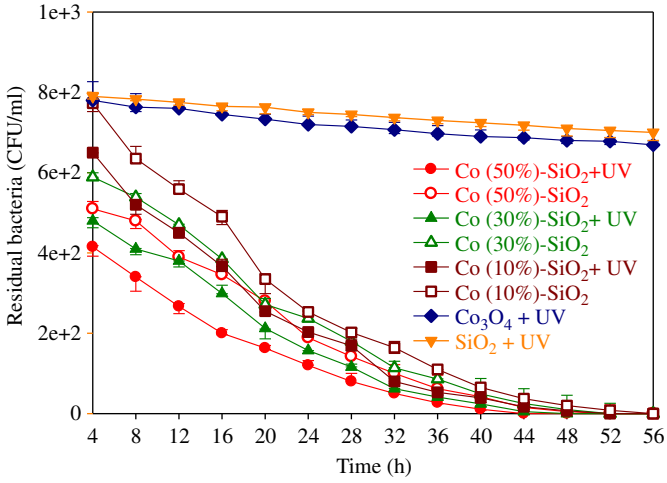

Fig. 5. Plot of the survival number of *E. coli* with different catalysts at 6 μg/ml concentration under UV illumination and dark condition. Data are shown from triplicate experiments.

3.3.4. Effect of the catalyst concentration

Various concentrations of different powders were examined for inhibition studies to determine MIC. In the Co-doped nanoparticle free medium, no inhibition effect was observed after UV light exposure due to low energy UV-A irradiation. For Co-doped SiO_2 samples, the MIC against *S. aureus* was found to be 3 μg/ml where as that of *E. coli* was found to be 1 μg/ml. The different MIC values for certain sample indicated its different toxicity against the Gram-positive *S. aureus* and Gram-negative *E. coli* strains. With the increase in the concentration of Co-doped SiO_2 solution, the inhibition efficiency has also been increased so that at higher concentrations (up to 6 μg/ml), the growth of bacteria was completely inhibited in both cases.

There are many studies about the MIC for various antibacterial agents, with different results for different microorganisms. MIC is dependent of many factors and the non-standardized procedures make difficult to compare its results from one report to another. It is worthy to note these four concentrations of catalysts have been chosen due to clear difference between CFU results for both microorganisms at given condition. For example, there was no significant difference in CFU at 1 and 2 μg/ml catalyst concentration for *E. coli* and in CFU at 5 and 6 μg/ml catalyst concentration for *S. aureus*. In addition, no bactericide efficiency was observed at 0.5 μg/ml concentration for all catalysts.

3.3.5. Effect of the microorganism

The nanoparticle powders were found to have a strong antibacterial activity regardless of Gram classes, though they were more efficient against Gram-negative bacterium. Since a lower MIC is an indication of a better antimicrobial agent, it is expected that Co-doped SiO_2 samples was found to have more effective antibacterial activity against *E. coli* as shown in Fig. 6. The difference between the antibacterial effect of samples against *E. coli* and *S. aureus* could be explained by microorganism structural difference in Gram-negative and Gram-positive bacteria. Both bacteria have similar internal, but different external structures. A Gram-positive bacterium has a thick peptidoglycan layer that contains teichoic and lipoteichoic acids. A Gram-negative bacterium has a thin peptidoglycan layer and an outer membrane that contains lipopolysaccharide, phospholipids, and proteins. Thus, *S. aureus* needs longer contact time or higher catalyst concentrations to achieve the same effect as *E. coli*.

3.3.6. Effect of the time

In addition, the important factor affecting the antibacterial effect is the contact time of the microorganisms suspended in water with catalyst powder. With the increase of contact time, the numbers of viable cells of both microorganisms, *E. coli* and *S. aureus*, decreased. As shown in Fig. 5, for *E. coli*, the contact time needed to kill nearly all the viable cells was 40, 44 and 46 h with Co (50%)-SiO_2, Co (30%)-SiO_2 and Co (10%)-SiO_2, respectively, at 6 μg/ml catalyst concentration under UV illumination. For *S. aureus*, the same effect was obtained after contact for 44, 46 and 48 h with Co (50%)-SiO_2, Co (30%)-SiO_2 and Co (10%)-SiO_2, respectively, at the same condition.

3.3.7. Effect of the illumination

It is seen from Fig. 5 that the bacteria inactivation was obtained under both UV light and dark conditions with higher efficiency in former case. However, the photochemical inactivation (in the absence of any catalyst) was negligible due to low energy UV-A illumination. The photocatalytic microbial inactivation has been reported in number of studies for different microorganisms and cell cultures. It was explained by different mechanisms such as cell membrane and the wall damage [27–29], physicochemical alteration of the cell membrane [30], promotion of cell membrane permeability to Ca^{2+} [31], reduction of intracellular superoxide dismutase activity (a protective enzyme from oxidative stress) [32] and abnormal cell division [30]. Hydroxyl radical has been reported as the major oxidant [33–35] but, other reactive oxygen species, such as H_2O_2, O_2^{2-} and O_2^- were also shown responsible of oxidation [36–38]. Under UV light, disruption of bacteria cell surface are attained by exposure to reactive oxygen species generated by photocatalysis; in the dark, microbicidal effects of metal ions released from solid matrix and penetrated into bacterial cell membranes may inhibit the bacteria growth. However, it is reported that oxygen dissolved in the solution can generate superoxide anions by single-electron reduction which does not require UV irradiation [39,40].

4. Catalyst recovery and reuse

Catalyst deactivation is one of the drawbacks on the application of photocatalytic degradation processes, deposition of photoinsensitive species on the photocatalyst surface blocking its active sites. At present work, the used powder catalysts were regenerated by treating with boiling distilled water and then by drying in a hot air oven at a temperature of 100 °C. The catalysts under consideration have not shown a

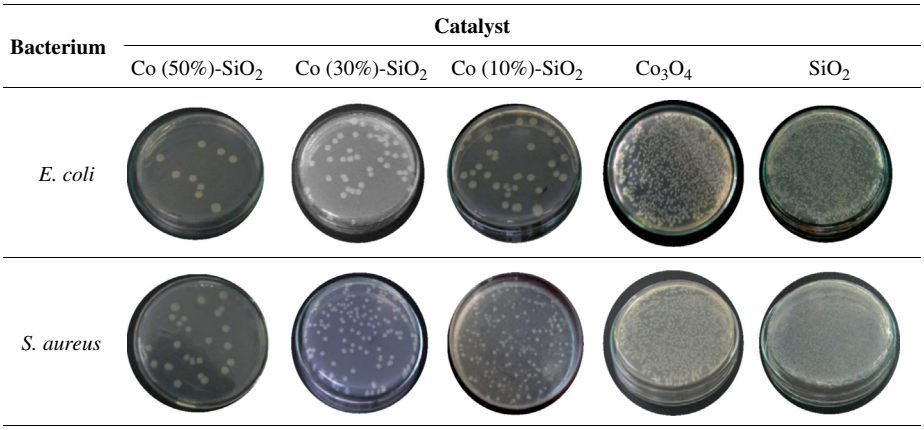

Fig. 6. Photographs showing bacterial colonies in plates after 40 h under UV illumination in the presence of 6 μg/ml Co (50%)-SiO_2 catalyst powder.

significant decrease in their photoinduced and dark microbiocide efficiency when the antimicrobial experiments were repeated three times using the same samples. The reproducibility of experimental data is shown in Fig. 5.

5. Conclusion

Nano-SiO_2 can be used as a carrier to prepare inorganic antibacterial materials. Novel Co-doped SiO_2 nanopowders were prepared via solvothermal process. The morphology, crystallinity and optical properties of the synthesized nanoparticles were analyzed by SEM micrographs, XRD patterns and UV–vis spectra, respectively. Despite that the single component SiO_2 and Co_3O_4 nanoparticles had no effect on the inhibition growth; Co-doping resulted to the excellent antibacterial properties against *E. coli* and *S. aureus*. The antibacterial efficiency was affected by size, chemical composition, structural and optical characteristics of catalysts and tested microorganisms type. Our results clearly demonstrated the antibacterial activity even in the absence of UV light.

Acknowledgments

The authors would like to acknowledge financial support from Islamic Azad University, Shahreza Branch.

References

[1] L. Slutsker, S.F. Altekruse, D.L. Swerdlow, Foodborne diseases: emerging pathogens and trends, Infectious Disease Clinics of North America 12 (1998) 199–216.
[2] P.G. Luo, F.J. Stutzenberger, Nanotechnology in the detection and control of microorganisms, Advances in Applied Microbiology 63 (2008) 145–181.
[3] W. Jiang, H. Mashayekhi, B. Xing, Bacterial toxicity comparison between nano and micro-scaled oxide particles, Environmental Pollution 157 (2009) 1619–1625.
[4] X. Hu, S. Cook, P. Wang, H.-M. Hwang, In vitro evaluation of cytotoxicity of engineered metal oxide nanoparticles, Science of the Total Environent 407 (2009) 3070–3072.
[5] A. Top, S. Ülkü, Silver, zinc, and copper exchange in a Na-clinoptilolite and resulting effect on antibacterial activity, Applied Clay Science 27 (2004) 13–19.
[6] A.M.P. McDonnell, D. Beving, A. Wang, W. Chen, Y. Yan, Hydrophilic and antimicrobial zeolite coatings for gravity-independent water separation, Advanced Functional Materials 15 (2005) 336–340.
[7] I. Satoshi, Antibacterial properties of resin composites and dentin bonding systems, Dental Materials 19 (2003) 449–457.
[8] L. Zhang, J.C. Yu, H.Y. Yip, Q. Li, K.W. Kwong, A.W. Xu, P.K. Wong, Ambient light reduction strategy to synthesize silver nanoparticles and silver-coated TiO_2 with enhanced photocatalytic and bactericidal activities, Langmuir 19 (2003) 10372–10380.
[9] S. Zhang, R. Fu, D. Wu, W. Xu, Q. Ye, Z. Chen, Preparation and characterization of antibacterial silver-dispersed activated carbon aerogels, Carbon 42 (2004) 3209–3216.
[10] A. Oya, T. Banse, F. Ohashi, S. Otani, An antimicrobial and antifungal agent derived from montmorillonite, Applied Clay Science 6 (1991) 135–142.
[11] E. Vernè, S.D. Nunzio, M. Bosetti, P. Appendino, C.V. Brovarone, G. Maina, M. Cannas, Surface characterization of silver-doped bioactive glass, Biomaterials 26 (2005) 5111–5119.
[12] V. Hornebecq, M. Antonietti, T. Cardinal, M. Treguer-Delapierre, Stable silver nanoparticles immobilized in mesoporous silica, Chemistry of Materials 15 (2003) 1993–1999.
[13] K. Yamamoto, S. Ohashi, M. Aono, T. Kokubo, I. Yamada, J. Yamauchi, Antibacterial activity of silver ions implanted in SiO_2 filler on oral streptococci, Dental Materials 12 (1996) 227–229.
[14] B. Gao, X. Zhang, J. Wang, Preparation and antibacterial characteristic of water-insoluble antibacterial material QPEI/SiO_2, Journal of Materials Science: Materials in Medicine 19 (9) (2008) 3021–3028.
[15] A. Erkan, U. Bakir, G. Karakas, Photocatalytic microbial inactivation over Pd doped SnO_2 and TiO_2 thin films, Journal of Photochemistry and Photobiology A: Chemistry 184 (2006) 313–321.
[16] J. Husheng, H. Wensheng, W. Liqiao, X. Bingshea, L. Xuguang, The structures and antibacterial properties of nano-SiO_2 supported silver/zinc–silver materials, Dental Materials 24 (2008) 244–249.
[17] N. Talebiana, M.R. Nilforoushan, E. Badri Zargar, Enhanced antibacterial performance of hybrid semiconductor nanomaterials: ZnO/SnO_2 nanocomposite thin films, Applied Surface Science 258 (2011) 547–555.
[18] M.G. Nair, M. Nirmala, K. Rekha, A. Anukaliani, Structural, optical, photocatalytic and antibacterial activity of ZnO and Co doped ZnO nanoparticles, Materials Letters 65 (2011) 1797–1800.
[19] T. Amna, M. Shamshi Hassan, M. Pandurangan, M.-S. Khil, H.-K. Lee, I.H. Hwang, Characterization and potent bactericidal effect of cobalt doped titanium dioxide nanofibers, Ceramics International 39 (3) (2013) 3189–3193.
[20] L. Eddie, C. Simmers, D. Andrew Knight, Cobalt complexes as antiviral and antibacterial agents, Pharmaceuticals 3 (2010) 1711–1728.

[21] Z. Wang, Y.-H. Lee, B. Wu, A. Horst, Y. Kang, Y.J. Tang, D.-R. Chen, Anti-microbial activities of aerosolized transition metal oxide nanoparticles, Chemosphere 80 (5) (2010) 525–529.

[22] T. Nagano, S. Fujisaki, K. Sato, K. Hataya, Y. Iwamoto, M. Nomura, S.I. Nakao, Relationship between the mesoporous intermediate layer structure and the gas permeation property of an amorphous silica membrane synthesized by counter diffusion chemical vapor deposition, Journal of American Ceramic Society 91 (2008) 71–76.

[23] F. Gu, C. Li, Y. Hu, L. Zhang, Synthesis and optical characterization of Co_2O_3 nanocrystals, Journal of Crystal Growth 304 (2007) 369–373.

[24] N. Zhang, Y. Gao, H. Zhang, X. Feng, H. Cai, Y. Liu, Preparation and characterization of core-shell structure of SiO_2@Cu antibacterial agent, Colloids and Surfaces B: Biointerfaces 81 (2) (2010) 537–543.

[25] N. Jones, B. Ray, K.T. Ranjit, A.C. Manna, FEMS: antimicrobial activities of commercial nanoparticles against an environmental soil microbe, *Pseudomonas putida* KT2440, Microbiological Letters 279 (2008) 71–76.

[26] N.M. Franklin, N.J. Rogers, S.C. Apte, G.E. Batley, G.E. Gadd, P.S. Casey, Comparative toxicity of nanoparticulate ZnO, bulk ZnO, and $ZnCl_2$ to a freshwater microalga (*Pseudokirchneriella subcapitata*): the importance of particle solubility, Environmental Science and Technology 41 (2007) 8484–8490.

[27] V.A. Nadtochenko, A.G. Rincon, S.E. Stanca, J. Kiwi, Dynamics of *E. coli* membrane cell peroxidation during TiO_2 photocatalysis studied by ATR-FTIR spectroscopy and AFM microscopy, Journal of Photochemistry and Photobiology A: Chemistry 169 (2005) 131–137.

[28] H.L. Liu, T.C.K. Yang, Photocatalytic inactivation of *Escherichia coli* and *Lactobacillus helveticus* by ZnO and TiO_2 activated with ultraviolet light, Process Biochemistry 39 (4) (2003) 475–481.

[29] K. Sunada, T. Watanabe, K. Hashimoto, Studies on photokilling of bacteria on TiO_2 thin film, Journal of Photochemitry and Photobiology A: Chemistry 156 (2003) 227–233.

[30] P. Amezaga-Madrid, R. Silveyra-Morales, L. Cordoba-Fierro, G. V. Nevarez-Moorillon, M. Miki-Yoshida, E. Orrantia-Borunda, F. J. Solis, Journal of Photochemistry and Photobiology B: Biology 70 (2003) 45–50.

[31] H. Sakai, E. Ito, R. Cai, T. Yoshioka, Y. Kubota, K. Hashimoto, A. Fujishima, Intracellular Ca^{2+} concentration change of T24 cell under irradiation in the presence of TiO_2 ultrafine particles, Biochimica et Biophysica Acta General Subjects 1201 (1994) 259–265.

[32] Y. Koizumi, R Yamada, M. Nishioka, Y. Matsumura, T. Tsuchido, M. Taya, Deactivation kinetics of *Escherichia coli* cells correlated with intracellular superoxide dismutase activity in photoreaction with titanium dioxide particles, Journal of Chemical Technology and Biotechnology 77 (2002) 671–677.

[33] J.C. Sjorgen, R.A. Sierks, Inactivation of phage MS2 by iron-aided TiO_2 photocatalysis, Applied Environmental Microbiology 60 (1994) 344–347.

[34] R.J. Watts, S. Kong, M.P. Orr, G.C. Miller, B.E. Henry, Photocatalytic inactivation of coliform bacteria and viruses in secondary wastewater effluent, Water Research 29 (1995) 95–100.

[35] J.C. Ireland, P. Klostermann, E.W. Rice, R.M. Clark, Inactivation of *Escherichia coli* by titanium dioxide photocatalytic oxidation, Applied Environmental Microbiology 59 (1993) 1668–1670.

[36] P.C. Maness, S. Smolinski, D.M. Blake, Z. Huang, E.J. Wolfrum, W. A. Jacoby, Bactericidal activity of photocatalytic TiO_2 reaction: toward an understanding of its killing mechanism, Applied Environmental Microbiology 65 (1999) 4094–4098.

[37] Y. Kikuchi, K. Sunada, T. Iyoda, K. Hashimoto, A. Fujishima, Photocatalytic bactericidal effect of TiO_2 thin films: dynamic view of the active oxygen species responsible for the effect, Journal of Photochemistry and Photobiology A: Chemistry 106 (1997) 51–56.

[38] T.L. Xu, P.V. Kamat, K.E. O'Shea, Mechanistic evaluation of arsenite oxidation in TiO_2 assisted photocatalysis, Journal of Physical Chemistry A 109 (40) (2005) 9070–9075.

[39] K. Hirota, M. Sugimoto, M. Kato, K. Tsukagoshi, T. Tanigawa, H. Sugimoto, Preparation of zinc oxide ceramics with a sustainable antibacterial activity under dark conditions, Ceramics International 36 (2010) 497–506.

[40] L. Huang, D.Q. Li, Y.-J. Lin, M. Wei, D.G. Evans, X. Duan, Controllable preparation of Nano-MgO and investigation of its bactericidal properties, Journal of Inorganic Biochemistry 99 (2005) 986–993.